RSC Advances

PAPER

View Article Online
View Journal | View Issue

Cite this: *RSC Adv.*, 2021, **11**, 1969

Additive-free photo-mediated oxidative cyclization of pyridinium acylhydrazones to 1,3,4-oxadiazoles: solid-state conversion in a microporous organic polymer and supramolecular energy-level engineering†

Kyung-su Kim,[a] You Kyoung Chung,[a] Hyunwoo Kim,[a] Chae Yeon Ha,[a] Joonsuk Huh [abc] and Changsik Song *[a]

Received 11th November 2020
Accepted 22nd December 2020

DOI: 10.1039/d0ra09581h

rsc.li/rsc-advances

We discovered the efficient catalyst-free, photo-mediated oxidative cyclization reaction of bis-*p*-pyridinium benzoyl hydrazone (**BH1**) to 2-pyridinium-5-phenyl-1,3,4-oxadiazoles. This photoreaction is remarkable because it does not require additives (*e.g.*, bases, strong oxidants, or photocatalysts), which are essential in previous reports, and proceeds very effectively even with solid-state microporous organic polymers. Interestingly, we found that the inclusion complexation of **BH1** with cucurbit[7]uril (**CB7**) interferes with the photo-induced electron transfer from **BH1** to molecular oxygen through modification of the LUMO energy level, thus inhibiting the photo-medicated oxidative cyclization.

Introduction

Acylhydrazones are well known to be converted from the *E*-isomer to *Z*-isomer under visible or UV light irradiation, and reversibly return to the *E*-isomer by thermal treatment[1,2] (Fig. 1a). Moreover, acylhydrazones can be transformed to oxadiazole derivatives by the oxidative cyclization reaction under UV-irradiation including a photocatalyst or under the condition of using a strong oxidizing agent. 1,3,4-Oxadiazoles are an essential class of five-membered heterocyclic compounds that have been intensively studied for biological and medicinal applications.[3,4] There are two general methods for the construction of 1,3,4-oxadiazoles from acylhydrazones *via* oxidative cyclization. The first method for oxidative cyclization of acylhydrazones to 1,3,4-oxadiazole is to use strong oxidants such as Dess–Martin reagent, ceric ammonium nitrate, bis(trifluoroacetoxy)iodobenzene, (diacetoxyiodo)benzene, or (2,2,6,6-tetramethylpiperidin-1-yl)oxyl (TEMPO).[5–11] The second method is photo-driven oxidative cyclization using a photocatalyst.[12,13] However, these synthetic methods for 1,3,4-oxadiazoles suffer from by-product generation caused by harsh reaction conditions or the necessity for separation and purification steps. Thus, the development of facile, mild, and additive-free photo-mediated protocols for 1,3,4-oxadiazole seems highly demanding.

Herein, we discovered the photo-mediated oxidative cyclization of pyridinium acylhydrazone conjugates, which forms

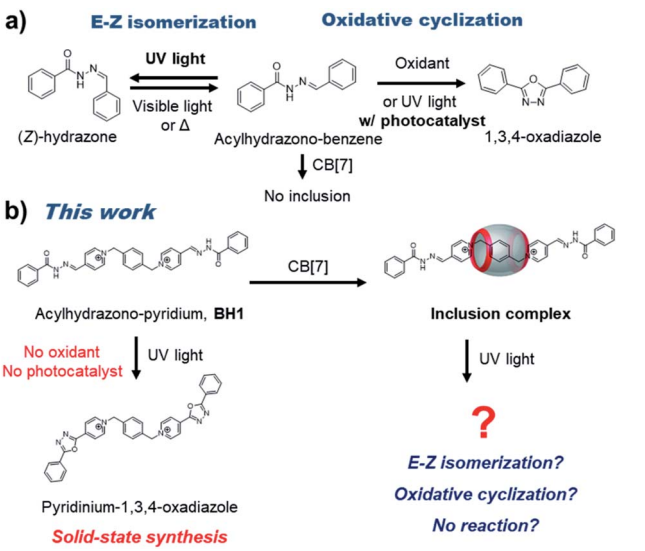

Fig. 1 (a) *E*–*Z* isomerization and oxidative cyclization of acylhydrazone. (b) Catalyst-free photo-mediated oxidative cyclization reaction of pyridinium acylhydrazone, and the effect of inclusion complexation on photoreaction.

[a]*Department of Chemistry, Sungkyunkwan University, 2066 Seobu-ro, Janan-gu, Suwon-si, Gyeonggi-do 16419, Republic of Korea. E-mail: songcs@skku.edu*

[b]*School of Advanced Institute of Nanotechnology, Sungkyunkwan University, Suwon 16419, Republic of Korea*

[c]*Institute of Quantum Biophysics, Sungkyunkwan University, Suwon 16419, Republic of Korea*

† Electronic supplementary information (ESI) available. See DOI: 10.1039/d0ra09581h

1,3,4-oxadiazole without additional additives (base, strong oxidant, or photocatalyst) (Fig. 1b). In our previous report,[14] bis-*p*-pyridinium benzoyl hydrazone (**BH1**, a cationic guest molecule) showed pH-dependent supramolecular assembly and dynamic covalent exchange reactions (transamination). Initially, we tested the effect of inclusion complexation of **BH1** with cucurbit[7]uril (**CB7**) to stimuli-responsiveness and self-assembly. Cucurbit[*n*]urils (**CB*n***), which consists of glycoluril units linked by methylene bridges, are considered to be suitable candidates for the complexation with cationic molecules because of their electronegative carbonyl functional groups and hydrophobic cavity with portals. Interestingly, the pyridinium acylhydrazone conjugate appeared to form well the inclusion complex with **CB7**, which affected its supramolecular polymerization. What is more interesting, however, is that the photo-mediated oxidative cyclization seems to be affected by the inclusion complexation, presumably *via* energy level modification. The **CB*n***-catalyzed or -templated photochemical reactions such as photohydrolysis[15] and photodimerizations[16–19] have been intensively investigated, but in most cases **CB*n*** promotes photoreaction by providing a cavity as a molecular container for effective spatial arrangement of reactants. On the other hand, the control of photoreaction through energy level tuning by encapsulation of reactants with **CB7**, not by spatial arrangement, is relatively rare and our work seems to provide with a noteworthy strategy to control photo-mediated chemical transformations.

Experimental

Materials

Pyridinium hydrazone conjugates, **H1** and **BH1** were prepared following the published procedures.[14] Cucurbit[7]uril (**CB7**) was purchased from CBTECH (Pohang, Korea). 1-Adamantanamine, benzohydrazide, 4-pyridinecarboxaldehyde, *p*-xylene dibromide, and iodomethane were commercially available and used as received.

Instruments

Ultraviolet-visible (UV-Vis) absorption data were acquired on a UV-1800 (Shimadzu) spectrophotometer in spectroscopic grade solvents without further purification. NMR measurements were performed in standard 5 mm NMR tubes at 300 K. All the data were acquired on a Bruker AVANCE III HD 500 and 700 MHz NMR spectrometer. Solid-state ^{13}C CP/MAS NMR spectra of **PH-MOP** and **Oxz-MOP** were recorded on a 400 MHz solid state NMR spectrometer (AVANCE III HD, Bruker, Germany) at KBSI Western Seoul center. Two-dimensional ROE spectra were measured with a spectral width of 8 kHz in 2 K data points using 16 scans for each of the 512 t_1 increments with 300 ms as a mixing time. Cyclic voltammetry (CV) was performed using an Epsilon electrochemical analyzer (EC Epsilon, BASi), and carried out in a three electrodes system, with Ag/Ag^+ as the reference electrode, Pt foil as the counter electrode, and the platinum working electrode, with a scan rate of 100 mV s^{-1}. For the photo-mediated oxidative cyclization reaction, pyridinium acylhydrazones were UV-irradiated with 342 nm using the Lumatec Superlite 410. Scanning electron microscopy (SEM) images were captured on a JEOL 7800 field emission SEM (FE-SEM) operated at an accelerating voltage of 15 kV. FT-IR spectra were recorded using a spectrometer Vertex 70 (Bruker Optic, Billerica, MA, USA), equipped with a diamond ATR unit.

Synthesis of microporous organic polymer (MOP)

Pyridinium acylhydrazone based MOP was synthesized by ball milling method. Bis-(pyridinium aldehyde) **1** (1.0 g, 2.1 mmol) and benzene-1,3,5-tricarbohydrazide **2** (0.35 g, 1.4 mmol) were added to a 25 mL stainless steel vessel with two stainless steel balls (diameter 15 mm). The vessel containing the substrates was vibrated at 20 Hz for 60 min at room temperature. The reacted powder was collected and washed by DMSO, DMF, acetone and MeOH. Yield: 1.2 g (88%).

General procedure for the photosynthesis of 1,3,4-oxadiazole derivatives from H1, BH1, and PH-MOP

1,3,4-Oxadiazole derivatives were synthesized by photo-mediated oxidative cyclization reaction of pyridinium acylhydrazones (**H1**, **BH1** and **PH-MOP**). A pyridinium acylhydrazone was dissolved in DMSO (0.1 M) and then UV-irradiated with 342 nm for 4 h using the Lumatec Superlite 410. After completion of the reaction monitored by ^{1}H NMR analysis except **PH-MOP**, the solvent was reduced, and then the residue was recrystallized from DMSO. Yield: 18–33 mg (83–92%).

Synthesis of Oxa-H1. Oxa-H1 was obtained as a yellowish white powder by a general method of photosynthesis of 1,3,4-oxadiazole using **H1** (27 mg). Yield: 25 mg (92%). ^{1}H NMR (DMSO-d_6, 700 MHz): δ 9.24 (d, J = 6.6 Hz, 2H), 8.81 (d, J = 6.6 Hz, 2H), 8.27 (d, J = 7.2 Hz, 2H), 7.77–7.70 (m, 3H), 4.45 (s, 3H). ^{13}C NMR (DMSO-d_6, 175 MHz): δ 166.48, 161.37, 147.48, 137.60, 133.51, 130.10, 127.78, 124.57, 123.09, 48.71. HRMS (ESI^+) [$C_{14}H_{12}N_3O_1$]: calcd $[M]^+$ 238.0975, found: 238.0975.

Synthesis of Oxa-BH1. Oxa-BH1 was obtained as a yellow powder by a general method of photosynthesis of 1,3,4-oxadiazole using **BH1** (38 mg). Yield: 33 mg (87%). ^{1}H NMR (DMSO-d_6, 500 MHz): δ 9.44 (d, J = 6.9 Hz, 4H), 8.85 (d, J = 6.9 Hz, 4H), 8.24 (d, 6.9 Hz, 4H), 7.78–7.61 (m, 6H), 7.69 (s, 4H), 5.98 (s, 4H). HRMS (ESI^+) [$C_{34}H_{26}N_6O_2$]: calcd $[M + H]^+$ 551.2114, found: 551.2185.

Synthesis of Oxa-MOP. Oxa-MOP was obtained as a yellowish white powder by a general method of photosynthesis of 1,3,4-oxadiazole using **PH-MOP** (22 mg). Yield: 18 mg (83%). Solid state ^{13}C CP-MAS NMR (400 MHz, spinning speed of 14 kHz): δ 172.35, 164.13, 160.65, 150.06, 142.19, 134.69, 130.13, 62.17.

Computational calculations

To obtain the local geometries and UV-Vis spectra of the interested molecules, we performed density functional theory (DFT) calculations by using a hybrid functional B3LYP and 6-311+g* basis set implemented in Gaussian 16 program. We also used the escf module integrated into Turbomole 7.3 program utilizing the resolution of identity (RI) method under the Conductor-like Screening Model (COSMO) condition in order to

consider a DMSO-solvent-mediated effect for the excited state calculations.

Results and discussion

Catalyst-free photo-mediated oxidative cyclization of pyridinium acylhydrazones to 1,3,4-oxadiazoles

In order to investigate the photo-reactivity of pyridinium acylhydrazones such as *E*–Z isomerization, we performed the time-dependent UV-irradiation (342 nm) experiment for methylpyridinium benzoyl hydrazone **H1** (0.66 mM in DMSO) (Fig. 2a). **H1** can be considered as a model for **BH1** since it is a dimer of **H1** with a 1,4-phenylene linker. Upon the UV-irradiation of **H1** solution, we observed that the UV-Vis absorption band of **H1** became blue-shifted (~19 nm), and the intensity of the absorption band at 348 nm considerably decreased (Fig. S1†). Of note, similar changes of optical properties can be observed during the *E*–*Z* isomerization process of acylhydrazones.[1,2] However, after performing thermal treatment and visible light irradiation experiments, we can confirm that a certain irreversible photoreaction occurred that was not *E*–*Z* isomerization. Fig. 2b shows the ^{1}H NMR spectra of **H1** (0.66 mM in DMSO) under UV-irradiation. After UV-irradiation for 1 h, the initial proton signals for **H1** decreased, and at the same time several new proton peaks were observed in the spectra. After UV-irradiation for 2 h, the proton peaks of **H1** completely disappeared, and only the newly observed peaks remained. We confirmed that **H1** changed to 2-methylpyridinium-5-phenyl-1,3,4-oxadiazole (**Oxa-H1**) by UV-irradiation using ^{1}H (Fig. S2†) and ^{13}C NMR (Fig. S3†), and high-resolution mass spectrometry (Fig. S4†) analyses. Similar with the case of **H1**, time-dependent UV-Vis absorption measurements and NMR experiments of **BH1** were also performed after UV-irradiation (342 nm). The UV-Vis absorption spectra of **BH1** (0.33 mM in DMSO) under UV-irradiation (Fig. S5†) showed blue-shifted absorption (~65 nm), which was similar to the patterns of **H1**, and they showed a more apparent isosbestic point at 295 nm. After the UV-irradiation of **BH1** for 2 h, the ^{1}H NMR spectra of **BH1** showed that the initial proton peaks of **BH1** disappeared and those of newly generated bis-*p*-(pyridinium 1,3,4-oxadiazole) (**Oxa-BH1**) remained (Fig. S6†).

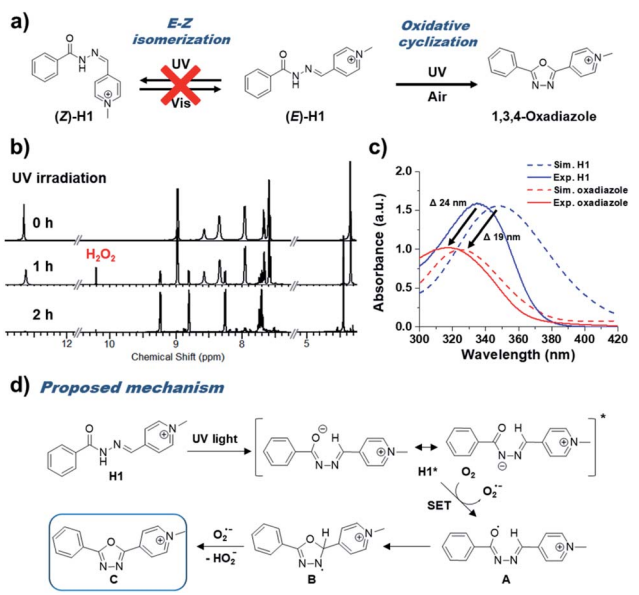

Fig. 2 (a) Catalyst-free photo-mediated oxidative cyclization from pyridinium acylhydrazones to 1,3,4-oxadiazoles. (b) Irradiation time-dependent ^{1}H NMR spectra of **H1** (500 MHz, 0.66 mM in DMSO-d_6). (c) Simulated and experimental UV-Vis absorption spectra of **H1** and 2-methylpyridinium-5-phenyl-1,3,4-oxadiazole. (d) Proposed mechanism of photo-mediated oxidative cyclization of pyridinium acylhydrazone, **H1**, to 1,3,4-oxadiazole.

Of note, this reaction is important because it has simple, economic, and environmental advantages compared to the previously reported methods for obtaining 1,3,4-oxadiazole from hydrazone. There is no need to worry about side reactions because the proposed approach does not use strong oxidizing agent; in addition, because no additional additives are used, less effort is required for purification. We expected that electronic modulation by the introduction of pyridinium into acylhydrazone would enable this additive-free photoreaction.

To support our experimental results observed by UV-Vis spectra and photoreaction, the DFT calculations of electronic states of **H1** and 1,3,4-oxadiazole in a DMSO solution were performed using B3LYP and 6-311+G* basis set (Fig. S7†). When **H1** was converted to 1,3,4-oxadiazole, a blue-shift of the absorption band (from 348 nm to 324 nm) similar to the experimental result was confirmed in simulated UV-Vis spectra (from 335 nm to 316 nm) (Fig. 2c). A possible mechanism of photo-mediated 1,3,4-oxadiazole synthesis from pyridinium acylhydrazone is represented in Fig. 2d. Upon the absorption of UV light, pyridinium acylhydrazone, **H1**, is excited to **H1***, which can be easily deprotonated owing to the electron-accepting ability of conjugated pyridinium to form a zwitterion. A single electron transfer (SET) from **H1*** to oxygen generates acyl radical **A**, which forms **B** by intramolecular cyclization. The generated superoxide radical anion ($O_2^{\bullet-}$) by SET from **H1*** attacks the proton of tertiary carbon of **B** to produce 1,3,4-oxadiazole, **C**. In fact, we confirmed the existence of superoxide radical anion ($O_2^{\bullet-}$) during the photo-mediated oxidative cyclization reaction by the observation of hydrogen peroxide in NMR spectra (10.2 ppm). It was observed that hydrogen peroxide was initially formed at the same level as the product 1,3,4-oxadiazole derivative in the photo-induced oxidative cyclization of **H1** (Fig. S2†). However, as shown in Fig. 2b, it appears that hydrogen peroxide decomposed over time under UV irradiation conditions, presumably due to photolysis of hydrogen peroxide. Of note, this oxidative cyclization reaction is carried out without additional strong oxidants or photocatalysts, which were necessary in previous studies.[5–13]

We attempted to apply the additive-free, photo-mediated oxidative cyclization method to the synthesis of oxadiazole-based microporous organic polymer (**Oxz-MOP**) under air. Our strategy is to obtain **Oxz-MOP** through a solid-state conversion of a pyridinium-acylhydrazone-based microporous organic polymer (**PH-MOP**), which can be prepared by facile condensation reaction between bis-(pyridinium aldehyde) **1** and

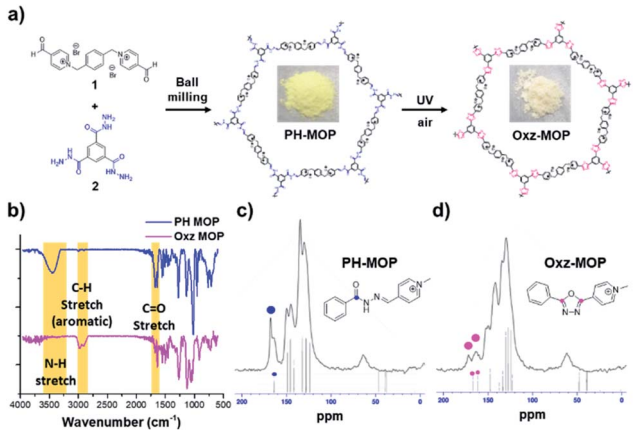

Fig. 3 (a) Synthesis of pyridinium acylhydrazone based microporous organic polymer (**PH-MOP**) by ball milling method, and 1,3,4-oxadiazole based MOP (**Oxz-MOP**) by photo-mediated oxidative cyclization of **PH-MOP** in the solid-state. (b) FT-IR spectra of **PH-MOP** (blue-line) and **Oxz-MOP** (pink-line). Solid-state ^{13}C CP/MAS NMR of (c) **PH-MOP** and (d) **Oxz-MOP**.

benzene-1,3,5-tricarbohydrazide **2**. Furthermore, we were able to synthesize **PH-MOP** successfully under ball milling condition at room temperature with a reactor frequency of 20 Hz for 1 h (Fig. 3a). Ball milling is a mechano-chemical method that has been considered an attractive tool for synthesizing various organic materials,[20,21] due to advantages such as environment-friendliness, fast speed and simplicity. The ^{13}C solid-state CP/MAS NMR spectra of **PH-MOP** revealed the similar patterns with that of **BH1** (Fig. S8†), which means that **PH-MOP** were well synthesized resulting from hydrazone formation reactions between **1** and **2**. Furthermore, to investigate the solid-state conversion of **PH-MOP** to oxadiazole-based microporous organic polymer (**Oxz-MOP**) by additive-free photo-mediated oxidative cyclization under air, we performed Fourier transform infrared (FT-IR) analysis of **PH-MOP** before and after UV-irradiation (Fig. 3b). In the FT-IR spectra of **PH-MOP** after UV-irradiation for 4 h, we could confirm that the disappearance of the N–H stretching peak at 3445 cm^{-1}, and decrease of the C=O stretching at 1681 cm^{-1}, which is consistent with the results with **BH1** (Fig. S9†). The ^{13}C solid-state CP/MAS NMR spectra of **PH-MOP** after UV-irradiation for 4 h supported also that photo-mediated conversion from **PH-MOP** to **Oxz-MOP** was occurred even in the solid state (Fig. 3c and d). Carbon signal of amide carbonyl carbon from **PH-MOP** at 167.7 ppm was changed to two broad peaks, which were speculated to originate from two carbons of 1,3,4-oxadiazole ring in **Oxz-MOP**. This photoreaction is noteworthy in that it provides a new bypass pathway to solve the difficulties in the synthesis and processing of aromatic poly(oxadiazole) due to the problem of poor solubility and high glass transition temperature (T_g).[22–26]

Inclusion complexation of BH1 with CB7 and inhibited photo-mediated oxidative cyclization reaction: mechanistic insight

Previously, our group reported bis-*p*-pyridinium benzoyl hydrazone **BH1** (Fig. 4), which exhibited a stimuli-responsive

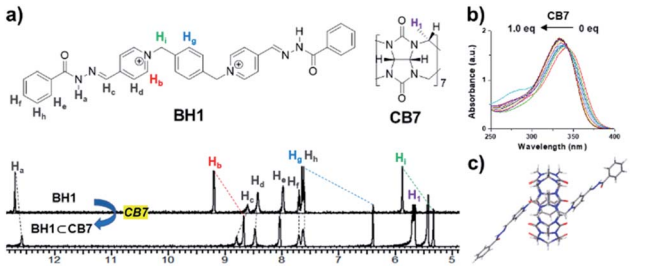

Fig. 4 (a) ^{1}H NMR spectra of **BH1** (500 MHz, 1.0 mM in DMSO-d_6) in the absence and presence of 1.0 equiv. of **CB7**. (b) UV-Vis absorption spectra of **BH1** in DMSO (0.33 mM) upon the addition of **CB7**. (c) Energy-minimized structure for **BH1⊂CB7** obtained by DFT calculation.

helical wire-type self-assembly by direct intermolecular interactions such as dipole–dipole, π–π, CH–π, and van der Waals interactions.[14] We tested whether **BH1** made an inclusion complex with **CB7** (Fig. 4a) and its effect on the photo-mediated oxidative cyclization. In the UV-Vis absorption spectra of **BH1** in DMSO (0.33 mM), the maximum absorption band initially at 340 nm showed a hypsochromic shift (~10 nm) and slightly increased absorptivity upon the addition of an increasing amount of **CB7** (Fig. 4b). This blue-shift in UV-Vis absorption spectra possibly originated from the changed microenvironment of **BH1** from bulk to macrocyclic upon encapsulation with **CB7**.[27,28]

^{1}H NMR titration experiments clearly showed the complexation event between **BH1** and **CB7**. **BH1** (1.0 mM in DMSO-d_6) was titrated against **CB7**, and ^{1}H NMR measurements were performed, which allowed to determine the equilibrium and binding constant (K) (Fig. 4a and S10†). Upon the addition of **CB7**, **BH1** formed only a 1 : 1 complex (Fig. S11†) with a considerable upfield shift in the protons of 1,4-xylylene and pyridinium, which indicated that **CB7** with shielding cavity make an internal complex with **BH1**.[29,30] Owing to the slow exchange in complexation between **CB7** and **BH1** on the NMR time scale, we monitored the amount of formed inclusion complexes, **BH1⊂CB7**, by integrating each NMR signal of a free and bound state of **BH1**. The binding constant (K) of **BH1** for **CB7** was calculated by fitting using eqn (1),[31] which allowed to determine the concentration of **BH1⊂CB7**, which was obtained by the multiplication of **BH1⊂CB7** fraction and total concentration of **BH1** ($[\mathbf{BH1}]_0$).

$$[\mathbf{BH1}\subset\mathbf{CB7}] = \frac{1}{2}\left([\mathbf{CB7}]_0 + [\mathbf{BH1}]_0 + \frac{1}{K_a}\right) - \sqrt{\left([\mathbf{CB7}]_0 + [\mathbf{BH1}]_0 + \frac{1}{K_a}\right)^2 + 4[\mathbf{CB7}]_0[\mathbf{BH1}]_0} \quad (1)$$

Compared to a previously study on the binding constant of the bis(pyridinium)-xylylene moiety with **CB7**,[32] we obtained a relatively lower K value ($1.53 \pm 0.82 \times 10^4$ M^{-1}), which was presumably due to solvent DMSO; this solvent fits better into

the cavity of a hydrophobic binding site than water.[33] To re-evaluate the binding affinity of **CB7** to **BH1**, the data obtained from UV-Vis titration experiments of **BH1** *versus* **CB7**, monitored at 330, 340, 360, 366, and 378 nm, were fitted according to the 1 : 1 binding isotherm on the website http://supramolecular.org (Fig. S12†),[34] which showed a similar binding constant (4.05×10^4 M^{-1}). The 2-D rotating-frame Overhauser effect spectroscopy (ROESY) NMR experiment was performed for the detailed structural characterization of inclusion complexes (**BH1**⊂**CB7**). As shown in Fig. S13,† ROE cross peaks between the proton of **CB7** (**H1**) and protons of bis(pyridinium)-1,4-xylylene on **BH1** (H_b and H_g) were clearly observed, which supported the formation of the 1 : 1 complex between **BH1** and **CB7**, in which **CB7** was symmetrically centrally positioned on **BH1**. Assuming 1 : 1 complexation, we were able to calculate the energy-minimized structure of the inclusion complex (**BH1**⊂**CB7**) in the ground state using the density functional theory (DFT) calculation at B3LYP/6-311+G*. As shown in Fig. 4c, centrally positioned **CB7** in the xylylene unit and Z-like structures with two anti-parallel planes of pyridium-acylhydrazone conjugates were observed. These structural characteristics have features that are similar to those in previous studies on inclusion complexation between the bis(pyridinium)-1,4-xylylene unit and **CB7**.[35,36]

UV-irradiation (342 nm) time-dependent UV-Vis absorption measurements and NMR experiments of **BH1**⊂**CB7** were performed. Inclusion complexes, **BH1**⊂**CB7** (0.33 mM in DMSO-d_6), which were prepared by the simple mixing of **BH1** (0.66 mM in DMSO-d_6) and **CB7** (0.66 mM in DMSO-d_6) solutions with 1 : 1 stoichiometry, were excited at 342 nm by UV-irradiation.

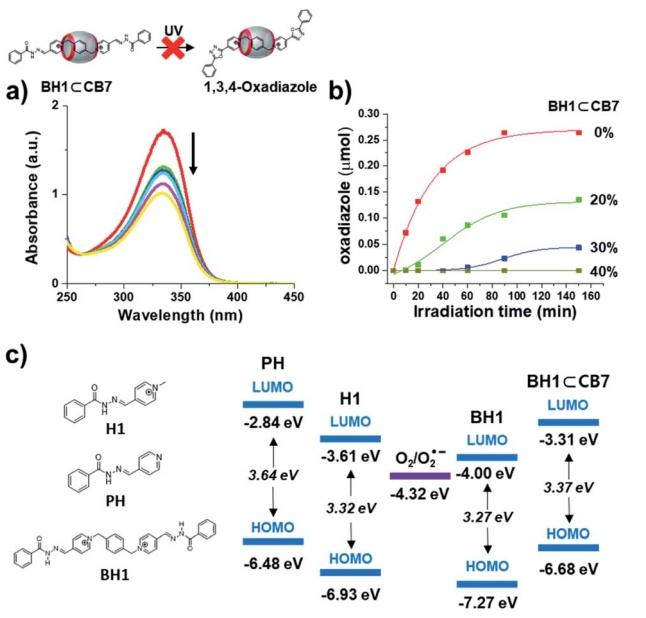

Fig. 5 (a) UV-Vis spectra of BH1⊂CB7 upon the 342 nm UV light irradiation (black arrows indicate the direction of absorptivity with an increase in irradiation time). (b) Amount of formed oxadiazole after the photo-mediated oxidative cyclization reaction. (c) The LUMO and HOMO energy diagram of PH, H1, BH1, and BH1⊂CB7, and the reduction potential of triplet oxygen.

Unlike the behavior in UV-Vis absorption spectra of **BH1** under UV light irradiation, the UV-Vis spectra of **BH1**⊂**CB7** did not show any shift in absorption band, isosbestic point, or increase in absorption at 275 nm (Fig. 5a). The ^{1}H NMR spectra of **BH1**⊂**CB7** (0.66 mM in DMSO-d_6), which were irradiated by UV light for 4 h, did not show a significant difference compared to the initial NMR spectra of **BH1**⊂**CB7** (Fig. S14†). Additional experiments on the photo-mediated oxidative cyclization reaction by varying the content of **BH1**⊂**CB7** in the solution of **BH1** were carried out (Fig. 5b and S15†). The UV-irradiation time-dependent ^{1}H NMR spectra of 20% content of **BH1**⊂**CB7** in the solution of **BH1** showed that only unbound **BH1** was changed to photo-reacted oxadiazole, while the total amount of bounded **BH1** (**BH1**⊂**CB7**) remained. However, for 40% content of **BH1**⊂**CB7** and above, we could not observe photo-reacted oxadiazole from **BH1** in ^{1}H NMR spectra, while the ratio of the amount of **BH1** and **BH1**⊂**CB7** was maintained. The isosbestic point, *i.e.*, the existence of an equilibrium between **BH1** and photo-reacted oxadiazole, was also not observed in UV-Vis spectra. Therefore, we concluded that **BH1** encapsulated into **CB7** was inhibited by the photo-mediated oxidative cyclization reaction, which also reduced the photo-reactivity of unbounded **BH1** (Fig. 5b).

We have not yet understood this phenomenon, but one thing to note is that in the presence of **BH1**⊂**CB7** there seems to be an induction period or retardation effect, which intensifies with increasing **CB7** content. Recently, Kaifer and coworkers reported the strong effect of the terminal carboxylate groups on the dissociation kinetics of bis(pyridinium)-xylylene[32] Through competitive binding analysis, the kinetic constants for dissociation were assessed; anionic carboxylates appear to act as a kinetic barrier to exchange reactions, but dissociation was much faster in the acid form of carboxyl groups. Similarly, an exchange experiment of **BH1**⊂**CB7** was performed with a competing guest molecule, adamantanamine (binding constant for **CB7**, $4.23 \pm 1.00 \times 10^{12}$ M^{-1}), using NMR titration (Fig. S16†). The NMR spectrum of **BH1**⊂**CB7** changed to that of **BH1** within 30 minutes after the addition of adamantanamine, indicating that **BH1** was completely exchanged to adamantanamine in the cavity of **CB7** and the exchange kinetics appeared very quickly. Thus, although the complex **BH1**⊂**CB7** is thermodynamically stable, it is kinetically labile so that the guest exchange can be relatively fast. These hypotheses require further investigation, but their relatively fast kinetics may influence the photo-mediated oxidative cyclization reaction of **BH1** in the presence of less than stoichiometric **CB7**. In other words, guest exchanges in the cavity of **CB7** between adjacent **BH1** molecules can occur at a relatively faster rate than oxidative cyclization reactions, thereby suppressing photo-mediated reactions below a stoichiometric amount.

To investigate the reason why photoreaction only occurred in pyridinium acylhydrazone conjugates (**H1** and **BH1**) and not in pyridine acylhydrazone conjugate (**PH**) (Fig. S17†) and inclusion complexes (**BH1**⊂**CB7**), and whether photoreaction was affected by their HOMO and LUMO energy levels, we measured the redox potentials of **H1**, **BH1**, **PH**, and **BH1**⊂**CB7** by cyclic voltammetry (Fig. S18†). The LUMO energy levels of **H1**, **BH1**,

PH, and **BH1**⊂**CB7** were obtained from reduction potentials at 1.19, 1.19, 1.96, and 1.43 V *vs.* Fc/Fc^+, respectively [$E_{LUMO} = -(E_{red} + 4.8\ V)$]. To calculate the HOMO energy level, their UV-Vis absorption spectra were used to estimate the HOMO–LUMO energy gap (ΔE). The calculated HOMO and LUMO energies of **H1**, **BH1**, **PH**, and **BH1**⊂**CB7** are shown in Fig. 5c. The LUMO energies of pyridinium acylhydrazones **H1** and **BH1** were −3.61 eV and −4.00 eV, respectively, which were significantly lower than those of pyridine acylhydrazone **PH** (−2.84 eV) and the inclusion complex **BH1**⊂**CB7** (−3.37 eV). All LUMO energies are slightly above the reduction potential for triplet oxygen (O_2) (−4.32 eV).

Based on the obtained redox potentials and the proposed mechanism for photo-induced electron transfer from acylhydrazone to O_2 (Fig. 2d), we could conclude that the electron transfer from photo-excited state to O_2 occurs much favourably in **H1** and **BH1** due to the small energy difference between their LUMO and the reduction potential of O_2, compared to the case of **PH** and **BH1**⊂**CB7**. According to Marcus theory, which explains the rate of electron transfer reactions between donor and acceptor, the electron transfer processes can be classified into three types of regions according to the rate constant *versus* reaction free energy: normal, activation-less, and inverted regions.[37–40] Among them, the 'inverted region' is where the electron transfer becomes slower down as the reaction becomes more exothermic. Apparently, it is consistent with the results of our system since the rate of photo-induced electron transfer seems slower as the energy gap becomes larger. It is likely that the photo-induced electron transfer occurs *via* 'inner sphere' mechanism or bonded electron transfer[41–44] through pre-organization of oxygen molecules and the excited **H1*** or **BH1***, although this hypothesis requires further investigation. It was noteworthy that in our additive-free photo-mediated oxidative cyclization reaction, the rate of electron transfer could be controlled by tuning the energy levels through structural variation and supramolecular approach (inclusion complexation).

Conclusions

We described the photo-mediated oxidative cyclization reaction of pyridinium acylhydrazones to 1,3,4-oxadiazole without a photocatalyst or strong oxidant. This photoreaction proceeded by single electron transfer from excited pyridinium acylhydrazones to molecular oxygen, generating superoxide radical anion (O_2^-). The photo-mediated oxadiazole formation reaction of pyridinium acylhydrazones proved effective even in solid-state microporous organic polymers. Moreover, the reaction could be completely inhibited by inclusion complexation with **CB7** *via* supramolecular engineering of LUMO energy levels.

Conflicts of interest

There are no conflicts to declare.

Acknowledgements

This work was supported by the Nano Material Development Program (2012M3A7B4049677) and Basic Science Research Programs (2019R1A2C1004256 and 2020R1A6A3A01100092) through the National Research Foundation of Korea (NRF) funded by the Ministry of Education, Science, and Technology, Republic of Korea. We also thank Prof. Ki Hyun Kim (School of Pharmacy, Sungkyunkwan University) for HRMS measurements.

Notes and references

1 B. Bai, M. Zhang, N. Ji, J. Wei, H. Wang and M. Li, *Chem. Commun.*, 2017, **53**, 2693–2696.
2 D. J. Van Dijken, P. Kovaricek, S. P. Ihrig and S. Hecht, *J. Am. Chem. Soc.*, 2015, **137**, 14982–14991.
3 F. A. Omar, N. M. Mahfouz and M. A. Rahman, *Eur. J. Med. Chem.*, 1996, **31**, 819–825.
4 A. S. Aboraia, H. M. Abdel-Rahman, N. M. Mahfouz and M. A. El-Gendy, *Bioorg. Med. Chem.*, 2006, **14**, 1236–1246.
5 C. Dobrota, C. C. Paraschivescu, I. Dumitru, M. Matache, I. Baciu and L. L. Ruta, *Tetrahedron Lett.*, 2009, **50**, 1886–1888.
6 P. Gao and Y. Y. Wei, *J. Chem. Res.*, 2013, 506–510.
7 S. Guin, T. Ghosh, S. K. Rout, S. A. Banerjee and B. K. Patel, *Org. Lett.*, 2011, **13**, 5976–5979.
8 C. C. Paraschivescu, A. G. Coman, C. C. Anghel and M. Matache, *Rev. Roum. Chim.*, 2015, **60**, 339–343.
9 M. Dabiri, P. Salehi and M. Baghbanzadeh, *Tetrahedron Lett.*, 2006, **47**, 6983–6986.
10 C. C. Paraschivescu, M. Matache, C. Dobrota, A. Nicolescu, C. Maxim, C. Deleanu, I. C. Farcasanu and N. D. Hadade, *J. Org. Chem.*, 2013, **78**, 2670–2679.
11 R. Y. Yang and L. X. Dai, *J. Org. Chem.*, 1993, **58**, 3381–3383.
12 B. Kurpil, K. Otte, M. Antonietti and A. Savateev, *Appl. Catal., B*, 2018, **228**, 97–102.
13 A. K. Yadav and L. D. S. Yadav, *Tetrahedron Lett.*, 2014, **55**, 2065–2069.
14 K.-s. Kim, H. J. Cho, J. Lee, S. Ha, S. G. Song, S. Kim, W. S. Yun, S. K. Kim, J. Huh and C. Song, *Macromolecules*, 2018, **51**, 8278–8285.
15 J. Smitka, A. Lemos, M. Porel, S. Jockusch, T. R. Belderrain, E. Tesarova and J. P. Da Silva, *Photochem. Photobiol. Sci.*, 2014, **13**, 310.
16 S. Y. Jon, Y. H. Ko, S. H. Park, H.-J. Kim and K. Kim, *Chem. Commun.*, 2001, 1938.
17 M. Pattabiraman, L. S. Kaanumalle, A. Natarajan and V. Ramamurthy, *Langmuir*, 2006, **22**, 7605.
18 N. Barooah, B. C. Pemberton and J. Sivaguru, *Org. Lett.*, 2008, **10**, 3339.
19 F. Biedermann, I. Ross and O. A. Scherman, *Polym. Chem.*, 2014, **5**, 5375.
20 M. K. Beyer and H. Clausen-Schaumann, *Chem. Rev.*, 2005, **105**, 2921–2948.
21 S. L. James, C. J. Adams, C. Bolm, D. Braga, P. Collier, T. Friscic, F. Grepioni, K. D. M. Harris, G. Hyett, W. Jones,

A. Krebs, J. Mack, L. Maini, A. G. Orpen, I. P. Parkin, W. C. Shearouse, J. W. Steed and D. C. Waddell, *Chem. Soc. Rev.*, 2012, **41**, 413–447.
22 S. Hsiao and G. Liou, *Polym. J.*, 2002, **34**, 917–924.
23 B. Schulz and E. Leibnitz, *Acta Polym.*, 1992, **43**, 343–347.
24 M. D. Losip, M. Bruma, I. Ronova, M. Szesztay and P. Muller, *Eur. Polym. J.*, 2003, **39**, 2011–2021.
25 S. Janietz and S. Anlauf, *Macromol. Chem. Phys.*, 2002, **203**, 427–432.
26 S. Janietz, S. Analauf and A. Wedel, *Synth. Met.*, 2001, **122**, 11–14.
27 G. Zhang, D. Gao, J. Chao, S. Shuang and C. Dong, *Dyes Pigm.*, 2009, **82**, 40–46.
28 D. Banik, J. Kuchlyan, A. Roy, N. Kundu and N. Sarkar, *J. Phys. Chem. B*, 2015, **119**, 2310–2322.
29 P. H. Dixit, R. V. Pinjari and S. P. Gejji, *J. Phys. Chem. A*, 2010, **114**, 10906–10916.
30 S. Li, H. Yin, G. Martinz, I. W. Wyman, D. Bardelang, D. H. Macartney and R. Wang, *New J. Chem.*, 2016, **40**, 3484–3490.
31 P. Thordarson, *Chem. Soc. Rev.*, 2011, **40**, 1305–1323.
32 I. Neira, M. D. Garcia, C. Peinador and A. E. Kaifer, *J. Org. Chem.*, 2019, **84**, 2325–2329.
33 C. Senac, S. Desgranges, C. Contino-Pepin, W. Urbach, P. F. J. Fuchs and N. Taulier, *ACS Omega*, 2018, **3**, 1014–1021.
34 D. Brynn Hibbert and P. Thordarson, *Chem. Commun.*, 2016, **52**, 12792–12805.
35 L. Mei, Z. N. Xie, K. Q. Hu, L. Y. Yuan, Z. Q. Gao, Z. F. Chai and W. Q. Shi, *Chem.–Eur. J.*, 2017, **23**, 13995–14003.
36 V. Sindelar, K. Moon and A. E. Kaifer, *Org. Lett.*, 2004, **6**, 2665–2668.
37 E. H. Yonemoto, G. B. Saupe, R. H. Schmehl, S. M. Hubig, R. L. Riley, B. L. Iverson and T. E. Mallouk, *J. Am. Chem. Soc.*, 1994, **116**, 4786–4795.
38 C. Turro, J. M. Zaleski, Y. M. Karabatsos and D. G. Nocera, *J. Am. Chem. Soc.*, 1996, **118**, 6060–6067.
39 H. Imahori, K. Tamaki, D. M. Guldi, C. P. Luo, M. Fujitsuka, O. Ito, Y. Sakata and S. Fukuzumi, *J. Am. Chem. Soc.*, 2001, **123**, 2607–2617.
40 M. Tachiya, *J. Phys. Chem.*, 1993, **97**, 5911–5916.
41 X. Amashukeli, N. E. Gruhn, D. L. Lichtenberger, J. R. Winkler and H. B. Gray, *J. Am. Chem. Soc.*, 2004, **126**, 15566–15571.
42 T. M. Bockman, Z. J. Karpinski, S. Sankararaman and J. K. Kochi, *J. Am. Chem. Soc.*, 1992, **114**, 1970–1985.
43 J. K. Kochi, *Acc. Chem. Res.*, 1992, **25**, 39–47.
44 S. J. Skoog and W. L. Gladfelter, *J. Am. Chem. Soc.*, 1997, **119**, 11049–11060.